relaxes to the ground singlet state (eq 6). Curves calculated on the basis of this mechanism are also shown in Figure 3. In these calculations it is assumed that 420-nm (Fe^{III}) absorption is independent of the Co^{II} spin state. The electron transfer from the Co^{II} $^2E(t_{2g}^6e_g)$ is spin permitted, but these results indicate that this process is comparatively slow. Equations 5 and 6 are equivalent to the electron transfer process that occurs when $Fe^{III}(CN)_6^{3-}$ reacts with Co^{II} chelate to form the paramagnetic bridged species Fe^{III}–CN–Co^{II} ($t_{2g}^5/t_{2g}^5e_g^2$). This undergoes intramolecular electron transfer to form the Fe^{II}–CN–Co^{III} ($t_{2g}^6/t_{2g}^5e_g$) product (eq 5). This product further undergoes high-spin to low-spin conversion to form the diamagnetic Fe^{II}–CN–Co^{III} species that is observed[9] (eq 6). The intersystem crossing ($^4T_1 \leftarrow {}^2E$) cannot be observed directly due to the low extinction coefficients of Co^{II}.

This system differs from other bimetallic electron transfer complexes where it is believed the electron proceeds via resonance transfer between metal centers with some influence from the bridging ligands of the ruthenium.[2,3] The MLCT ($Fe^{II} \rightarrow CN$) transition occurs in the near-UV, thereby ruling out this possibility. The rate of electron transfer has been found to be dependent on the polarity of the solvent system. In less polar solvent systems the electron transfer rates were found to be lower (Table III). This is interpreted as being due to small relative changes between cobalt and iron electronic energy levels. We propose that these shifts are due to changes in charge stabilization of the respective Fe^{II}–CN–Co^{III} and Fe^{III}–CN–Co^{II} species.

Registry No. $(NC)_5Fe^{II}CNCO^{III}$HEDTA, 83586-93-0; $(NC)_5Fe^{II}CNCO^{III}$NBETA, 83586-94-1.

Small-Angle X-ray Scattering by Nonaqueous Concentrated Electrolytes: $LiClO_4$ and $ZnBr_2$ in Ethyl Acetate

M. Nicolas* and E. Dartyge*

Contribution from the Laboratoire de Physique des Solides, Université de Paris-Sud, Centre d'Orsay, 91405 Orsay, France. *Received February 4, 1982*

Abstract: Small-angle X-ray scattering has been performed on concentrated nonaqueous electrolytes (i.e., $LiClO_4$– and $ZnBr_2$–ethyl acetate systems) for the first time. The very dilute solutions show a monotonic scattering, revealing a low degree of association between molecules of solute. For the most concentrated solutions a well-defined maximum is observed for a scattering vector $s = (10\ Å)^{-1}$ with $s = 2 \sin \theta/\lambda$. On increasing the salt concentration, the position of this maximum is shifted toward smaller angles, whereas the characteristic ring of the solvent is shifted toward higher angles, revealing structural changes.

A. Introduction

Recently X-ray and neutron scattering by concentrated aqueous solutions has had increasing experimental and theoretical attention.[1-5] Indeed, the diffraction experiments can provide extensive information about ion–solvent, ion–ion, and solvent–solvent interactions. In such aqueous systems, the scattering patterns reflect principally the ion–water interactions, whereas the ion–ion correlations are more difficult to show.[1] Nevertheless, the question of the existence of some ordered structure in concentrated electrolytes has been often raised.[1,4] The presence of a weak "prepeak" ($k \simeq 1\ Å^{-1}$ with $k = 4\pi \sin \theta/\lambda$) in the scattering patterns of aqueous systems seems to corroborate this hypothesis since it has been interpreted as due to some metal–metal interactions.[1,3,6,14] But it seems that water is not a good solvent in which to observe the ion–ion correlations. Its high dielectric constant ($\epsilon = 80$ at 293 K), principally due to numerous dipoles by unit volume, allows very strong ion–solvent interactions in the dilute range. (Indeed, water, a hydrogen-bonded solvent, has a very small size and a high dipole moment.) These interactions are still predominant on increasing the salt concentration, even though it has been shown that the dielectric constant of electrolytic solutions decreases[18] and that water undergoes important structural transformations.[8] Nevertheless, ion–ion interactions take place but often in a less important way. Thus, it seemed better to study nonaqueous solutions with a solvent of low dielectric constant (few dipoles by unit volume and large size of the molecule), allowing strong coulombic interactions. We chose ethyl acetate as solvent ($\epsilon = 6.09$ at 293 K). Indeed macroscopic data such as transport[7] and thermodynamic[8] properties of $LiClO_4$– (or $ZnBr_2$–) ethyl acetate solutions and microscopic data such as EXAFS[9] show that ionic clusters exist in this medium and that long-range ordered structures can be formed. In fact, the most important result of the EXAFS experiments performed on $ZnBr_2$–EtOAc solutions is that these ionic clusters involve nearly 100% of the total number of Zn^{2+} and Br^- ions even in the dilute range, whereas in water, for the saturated solution, only 60% of the ions are embedded in such aggregates and this ratio decreases quickly with dilution.[10] A first qualitative evaluation of the size of these clusters for concentrated ethyl acetate solutions has given an order of $\simeq 30$ Å. If such an estimate is valuable, one would expect to observe a specific scattering at small angles, typically for vectors $s \lesssim 9 \times 10^{-2}\ Å^{-1}$ ($s = 2 \sin \theta/\lambda$). For that reason, we performed small-angle X-ray-scattering experiments on these samples.

B. Experimental Section

a. Small-Angle Scattering. The absolute scattered intensity was measured with a spectrometer described elsewhere;[11] the intensity of the scattered radiation (monochromatic radiation Cu Kα, wavelength $\lambda = 1.54$ Å) was *collected* through a circular slit on a Si–Li detector protected by a beryllium window. The variation of the angle was obtained by varying the sample–detector distance, in constant steps. The thickness of the sample was controlled by various Teflon spacers; its optimum value

(1) J. E. Enderby and G. W. Neilson, *Adv. Phys.*, **29**, 323 (1980).
(2) J. E. Enderby, R. A. Howe, and W. S. Howells, *Chem. Phys. Lett.*, **21**, 1 (1973).
(3) E. Kalman and G. Palinkas, 31st Meeting of the International Society of Electrochemistry, Venice, Italy, Sept 22–26, 1980.
(4) M. P. Fontana, G. Maisano, P. Migliardo, and F. Wanderlingh, *J. Chem. Phys.*, **69**, 679 (1978).
(5) R. Caminiti, G. Licheri, G. Paschina, G. Piccaluga, and G. Pinna, *Z. Naturforsch, Teil A*, **35**, 1361–1367 (1980).
(6) J. E. Enderby and G. W. Neilson, *Rep. Prog. Phys.*, **44**, 593 (1981).
(7) M. Nicolas and R. Reich, *J. Phys. Chem.*, **85**, 2843 (1981).
(8) M. Nicolas and R. Reich, to be submitted for publication.
(9) A. Sadoc, A. Fontaine, P. Lagarde, and D. Raoux, *J. Am. Chem. Soc.*, **103**, 6287 (1981).
(10) P. Lagarde, A. Fontaine, D. Raoux, A. Sadoc, and P. Migliardo, *J. Chem. Phys.*, **72**, 3061 (1980).
(11) A. M. Levelut, M. Lambert, and A. Guinier, *C. R. Acad. Sci.*, **255**, 319 (1962).
(12) A. Guinier, "X-Ray Diffraction in Crystals, Imperfect Crystals and Amorphous Bodies", W. H. Freeman, San Francisco, 1963.

0002-7863/82/1504-7403$01.25/0

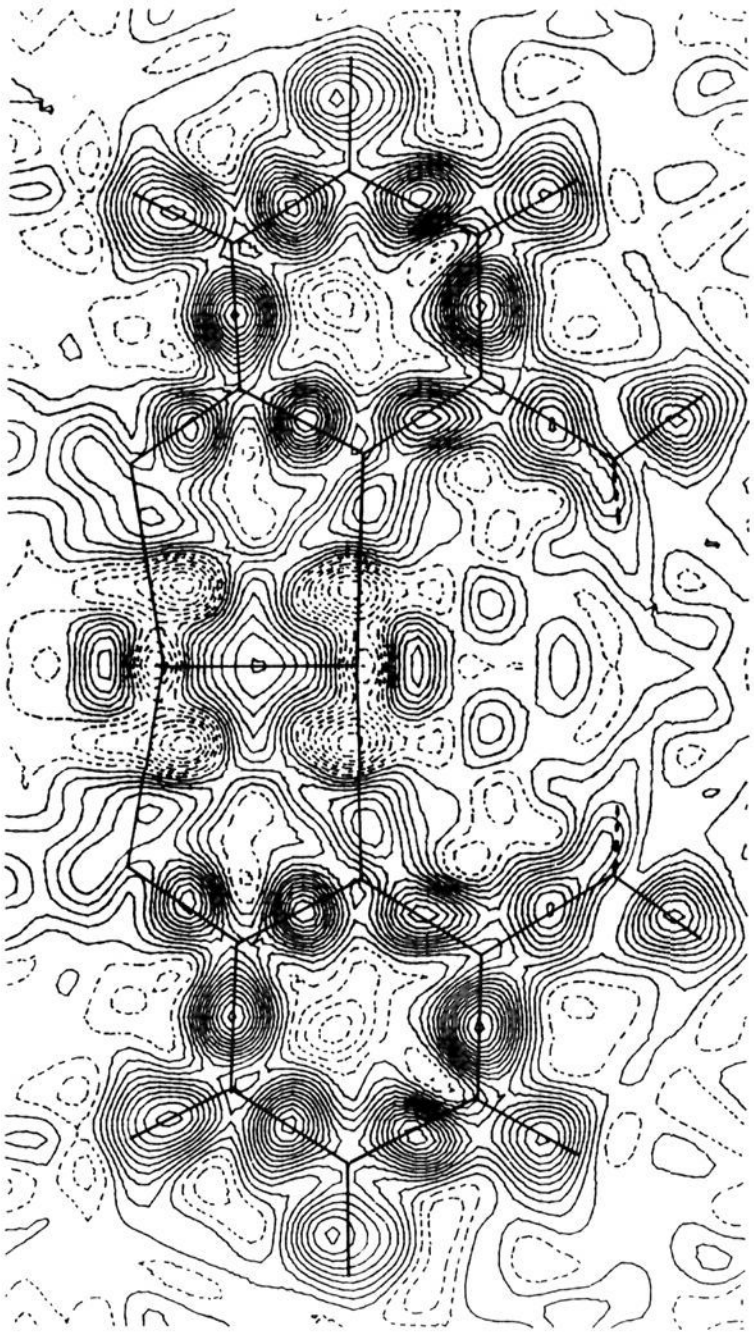

Figure 3. Average experimental deformation density in the plane of a wing (spacing of contours 0.05 e Å^{-3}).

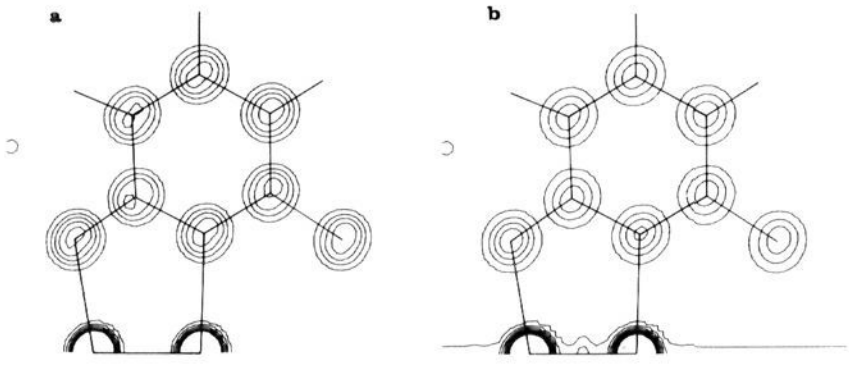

Figure 4. Estimated standard deviations of the experimental deformation density: (a) in the plane of one wing; (b) of the average deformation density (spacing of contours 0.025 e Å^3). Outside the atomic regions, and far from the Cr–Cr axis in (b), the esd is equal to 0.082 e Å^{-3} in (a) and 0.041 e Å^{-3} in (b). At the chromium positions the esd culminates at 0.6 e Å^{-3} (not all contours are shown). The esd of the error due to the spherical model used in the calculation of the scale factor was assumed to be 0.5% of the total density.

the direction of the Cr–Cr bond, which is therefore unreliable in the vicinity of each metal nucleus. In all other regions the errors may be assumed to be essentially random. Maps of the esd of the deformation density are shown in Figure 4, before and after averaging.[14] Clearly, in the second case the correlation between errors at averaged points needs to be considered.

Molecular Orbital Calculations

The theoretical density maps were obtained from ab initio LCAO–MO–SCF + CI calculations on $[H_2P(CH_2)_2]_4Cr_2$ carried out with the ASTERIX system of programs.[15] The Gaussian basis

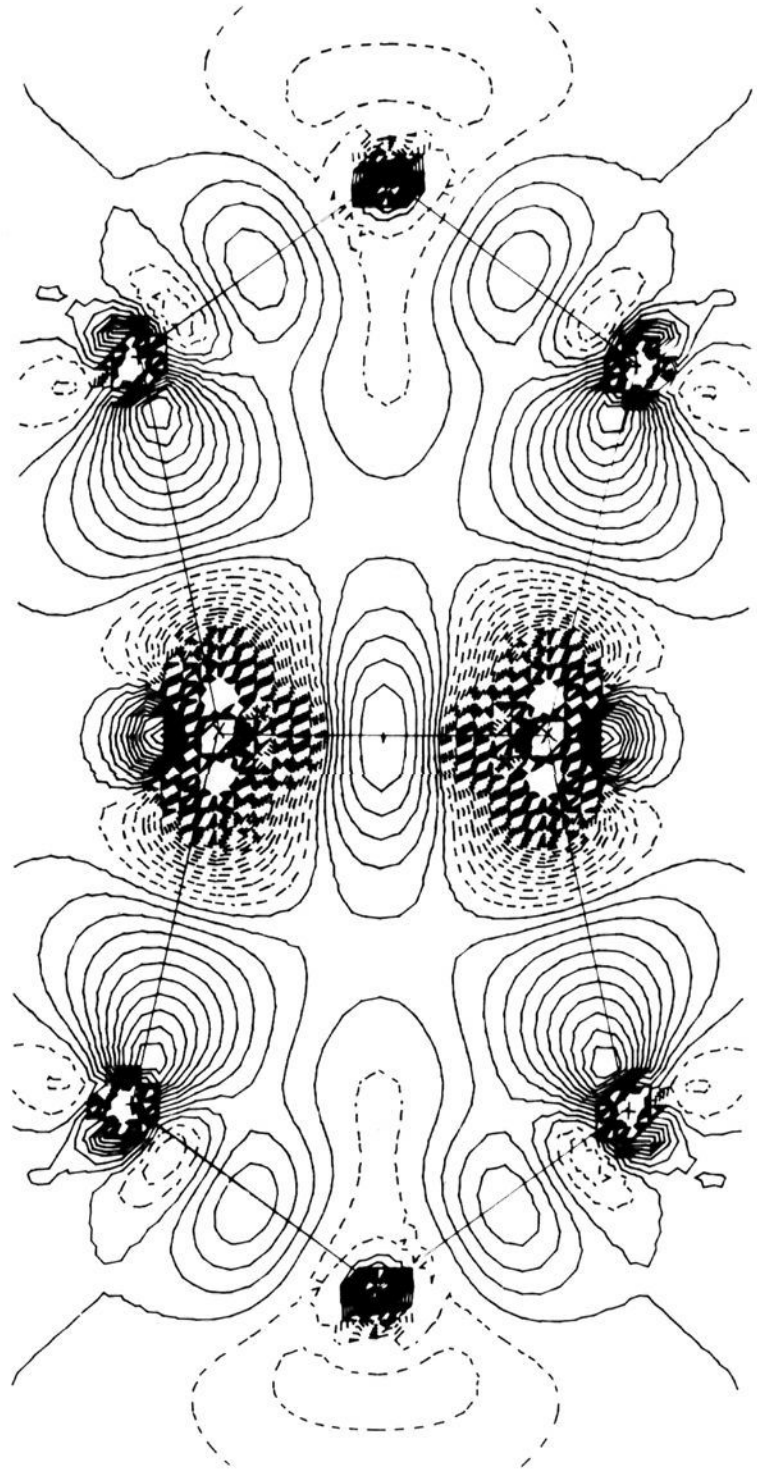

Figure 5. Theoretical deformation density in the plane of a wing (spacing of contours 0.05 e Å^{-3}).

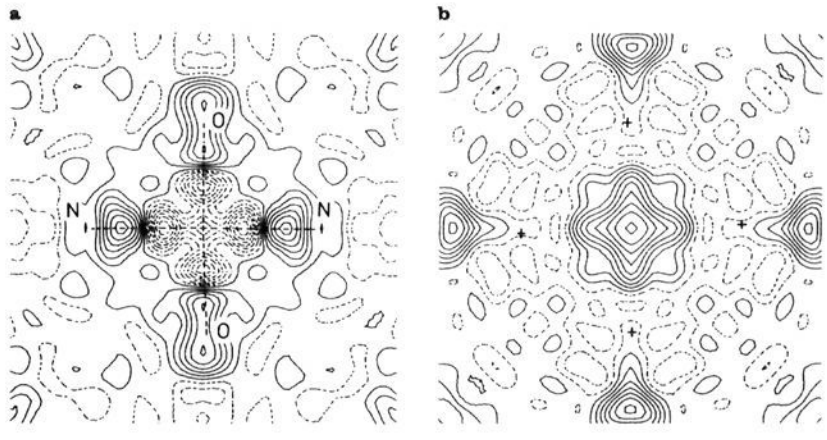

Figure 6. Average experimental deformation density in planes perpendicular to the Cr–Cr axis: (a) plane through the metal nucleus; (b) plane through the midpoint of the bond (spacing of contours 0.05 e Å^{-3}).

set used for Cr was taken from the (13,7,5) set of Hyla-Kryspin et al.[16] and incremented with one p function of exponent 0.15 and one diffuse d function of exponent 0.08. It was contracted to [5,3,3], that is, minimal for internal and 4p shells, double-ζ for 4 s shells, and triple-ζ for 3d shells. Basis sets (11,7), (9,5), and

(14) Rees, B. *Acta Crystallogr., Sect. A.* **1978**, *A34*, 254–256.

(15) Bénard, M.; Dedieu, A.; Demuynck, J.; Rohmer, M. M.; Strich, A.; Veillard, A.; Wiest, R. "ASTERIX: A System of Programs for the UNIVAC 1110" (unpublished). Bénard, M.; Barry, M. *Comput. Chem.* **1979**, *3*, 121–124.

(16) Hyla-Kryspin, I.; Demuynck, J.; Strich, A.; Bénard, M. *J. Chem. Phys.* **1981**, *75*, 3954–3961.

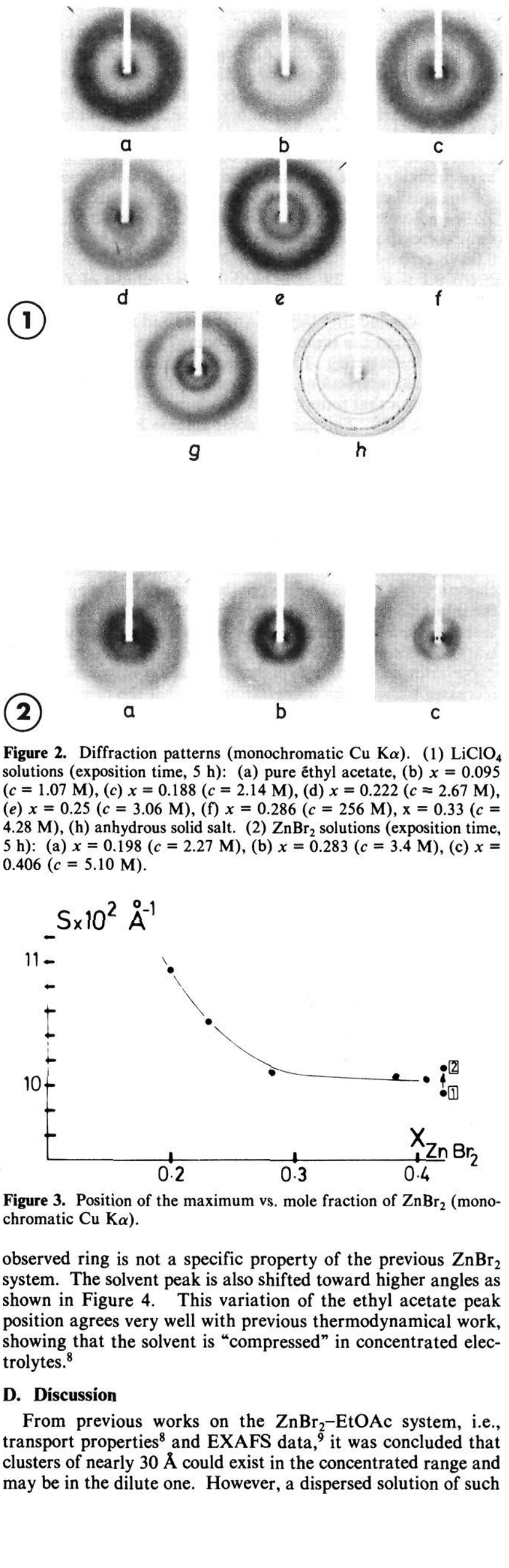

Figure 2. Diffraction patterns (monochromatic Cu Kα). (1) $LiClO_4$ solutions (exposition time, 5 h): (a) pure ethyl acetate, (b) $x = 0.095$ ($c = 1.07$ M), (c) $x = 0.188$ ($c = 2.14$ M), (d) $x = 0.222$ ($c = 2.67$ M), (e) $x = 0.25$ ($c = 3.06$ M), (f) $x = 0.286$ ($c = 256$ M), x = 0.33 ($c = 4.28$ M), (h) anhydrous solid salt. (2) $ZnBr_2$ solutions (exposition time, 5 h): (a) $x = 0.198$ ($c = 2.27$ M), (b) $x = 0.283$ ($c = 3.4$ M), (c) $x = 0.406$ ($c = 5.10$ M).

Figure 3. Position of the maximum vs. mole fraction of $ZnBr_2$ (monochromatic Cu Kα).

observed ring is not a specific property of the previous $ZnBr_2$ system. The solvent peak is also shifted toward higher angles as shown in Figure 4. This variation of the ethyl acetate peak position agrees very well with previous thermodynamical work, showing that the solvent is "compressed" in concentrated electrolytes.[8]

D. Discussion

From previous works on the $ZnBr_2$–EtOAc system, i.e., transport properties[8] and EXAFS data,[9] it was concluded that clusters of nearly 30 Å could exist in the concentrated range and may be in the dilute one. However, a dispersed solution of such

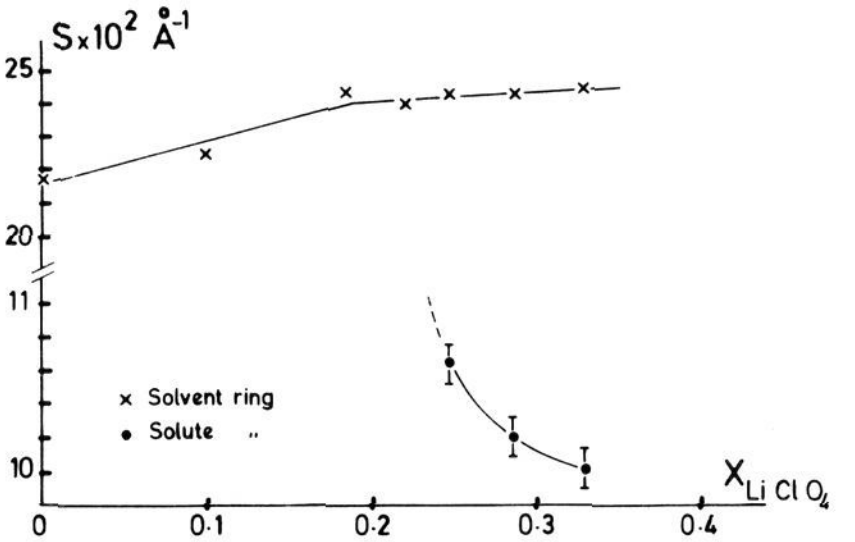

Figure 4. Position of both peaks (solution and solvent) vs. the mole fraction of $LiClO_4$ (monochromatic Cu Kα).

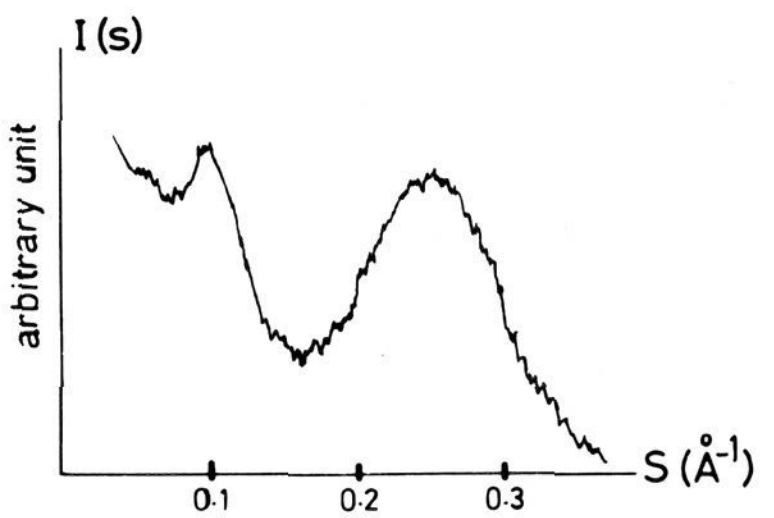

Figure 5. X-ray intensity curve vs. scattering vector for the saturated $LiClO_4$–EtOAc system.

aggregates would give at small angles a decreasing scattering intensity as a function of the wave vector $\boldsymbol{s}$. If some correlation exists between them, a maximum would occur for $\boldsymbol{s} \simeq 8 \times 10^{-2}$ Å^{-1}. Such a phenomenon is not observed down to $\boldsymbol{s} \simeq 3 \times 10^{-2}$ Å^{-1} since for low solute concentrations, i.e., $x \lesssim 0.1$, the monotonic Laue intensity is of the same order of magnitude as that of isolated $ZnBr_2$ molecules. However, if the clusters remain small, some interactions between them become likely with increasing solute concentration, and this fact must have some effect upon the experimental scattered intensity. (Indeed, our results show that the ratio p remains nearly equal to 1.5 in the very dilute range ($x \lesssim 0.0570 - c < 0.6$ M) but seems to decrease for higher concentrations (0.6 M $\lesssim c \lesssim 1$ M) (Table I).) Moreover, it must be noted that the average distance between isolated molecules is equal to 22 Å for $c = 0.15$ M ($x = 0.013$), to 14 Å for $c = 0.6$ M ($x = 0.057$), and to 11.8 Å for $c = 1$ M ($x = 0.091$). This mean distance must be compared with the location of the maximum ($\boldsymbol{s} \simeq (10$ Å$)^{-1}$) which appears with high intensity for $x \gtrsim 0.091$ (Figure 2).

The various experiments of small-angle X-ray (or neutron) diffraction which have been performed on concentrated aqueous electrolytes also reveal the existence of a weak peak, situated at $0.5 \lesssim \boldsymbol{k} \lesssim 1$ Å^{-1} ($\boldsymbol{k} = 4\pi \sin\theta/\lambda = 2\pi\boldsymbol{s}$), and several authors have assumed that it is due to metal–metal interactions.[1-6] Its position is shifted toward smaller angles at lower concentrations,[3,14,16] contrary to our observations on the ethyl acetate systems, where the well-defined peak is shifted toward higher angles.

(14) G. Maisano, P. Migliardo, F. Wanderlingh, M. P. Fontana, M. C. Bellissent-Funel, and M. Roth, *Solid-State Commun.*, **38**, 827 (1981).
(15) M. C. A. Donkersloot, *Chem. Phys. Lett.*, **57**, 561 (1978).
(16) A. Hyman and P. A. Vaughan in ref 13.
(17) A. M. Levelut and A. Guinier, *Bull. Soc. Fr. Mineral. Cristallogr.*, **90**, 445 (1967).
(18) H. Cachet, A. Cyrot, M. Fekir, and J. C. Lestrade, *J. Phys. Chem.*, **83**, 2419 (1979).

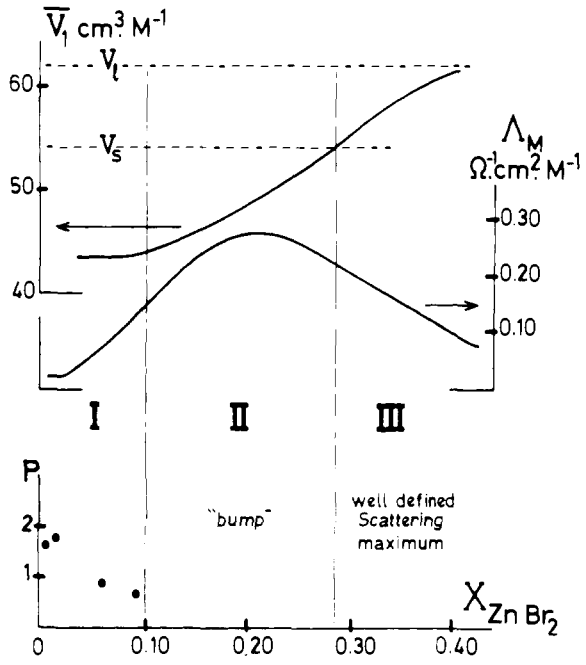

Figure 6. The three concentration ranges for the $ZnBr_2$–EtOAc system: V_1 = partial molar volume of solute, Λ_M = molar conductivity of solution, p = association degree determined by X-ray scattering.

On the other hand, another maximum has been observed recently, with very low contrast at $k \simeq 0.125$ Å^{-1} ($s \simeq 1.98 \times 10^{-2}$ Å^{-1}) by small-angle neutron scattering of $CuBr_2$, $NiCl_2$, and $ZnCl_2$ aqueous solutions,[14] and it has been attributed principally to the existence of correlated ordered domains with a correlation length of $\simeq$50 Å.

Up to now, it has been difficult to determine exactly the origin of the peak at $s = (10$ Å$)^{-1}$. Likely, both size effects and interparticles interactions can play a part in the scattering. But we can attempt to "visualize" the various structures which take place for various concentration ranges, taking into account the previous data obtained from thermodynamical or transport properties,[8] on the $ZnBr_2$–ethyl acetate system, for example, as shown in Figure 6.

(i) $x \lesssim 0.1$. Macroscopically, with increasing the solute concentration, the partial molar volume of $ZnBr_2$ remains constant and the molar conductivity Λ_M begins to increase sharply; this would mean that small charged particles are formed and that only their concentration (not their size) would increase. Microscopically, we observe a flat "monotonic" scattering revealing a low association degree between solute molecules and a randomly dispersed structure. Thus, in this concentration range, one would have probably some Zn^{2+} bounded to the –COO– group of the solvent, small conducting $(ZnBr_4)^{2-}$ or $(Zn_2Br_6)^{2-}$ ions, and neutral $ZnBr_2$ molecules since the associativity is only a mean value. But some correlations between particles begin to take place for $x \simeq 0.06$ ($c \simeq 0.6$ M).

(ii) $0.1 \lesssim x \lesssim 0.29$. The partial molar volume of $ZnBr_2$ increases up to the molar volume of anhydrous solid $ZnBr_2$, and the molar conductivity begins to decrease and then goes through a maximum; at the same time, a "bump" appears in the X-ray small-angle scattering. If this "prepeak" is interpreted as due to metal–metal interactions, this would mean that bigger clusters are formed or that some correlations between aggregates occur.

(iii) $x \gtrsim 0.29$. The partial molar volume V_1 reaches the 293 K extrapolated value of the molar volume of molten $ZnBr_2$, i.e., $V_1 = 61$ cm^3, and the conductivity is still decreasing, up to saturation. At the same time, a well-defined peak appears in the scattering patterns, situated at $s \simeq (10$ Å$)^{-1}$; its position is shifted toward lower angles on increasing the solute concentration, contrary to aqueous systems.[3] If the origin of this peak is attributed to metal–metal interactions, such behavior would suggest that the clusters would be less compact in the concentrated range than in the dilute domain; this phenomenon would corroborate the fact that the Zn–Br distance *increases* with salt concentration,[9] contrary to aqueous systems where it remains unchanged.[10]

Nevertheless, another hypothesis is that the size of the clusters increases with solute concentration and that the mean distance between them becomes of the same order of magnitude as their size. These two distinct hypothesis need a quantitative measurement of the scattered intensity to be developed.

Acknowledgment. The authors thank Dr. A. M. Levelut for fruitful discussions.

Registry No. $LiClO_4$, 7791-03-9; $ZnBr_2$, 7699-45-8; ethyl acetate, 141-78-6.